ELSEVIER

Grain size effect on multiple-stage transformations of a cold-rolled and annealed equiatomic TiNi alloy

S.H. Chang [a], S.K. Wu [a,b,*], G.H. Chang [b]

[a] *Department of Materials Science and Engineering, National Taiwan University, 1, Roosevelt Rd., Sec. 4, Taipei 106, Taiwan, ROC*
[b] *Department of Mechanical Engineering, National Taiwan University, Taipei 106, Taiwan, ROC*

Abstract

$Ti_{50}Ni_{50}$ shape memory alloy cold-rolled and annealed at specific conditions can exhibit a four-stage martensitic transformation. There are two small and two large peaks which are associated with the $B2 \rightarrow R \rightarrow B19'$ transformations of large grains in the specimen center and that of small grains near the rolling surface, respectively.
© 2005 Acta Materialia Inc. Published by Elsevier Ltd. All rights reserved.

Keywords: Shape memory alloy; Martensitic transformation; Cold working; Annealing; Differential scanning calorimetry

1. Introduction

TiNi alloys are known as the most important shape memory alloys (SMAs), with good shape memory effect (SME), superelasticity (PE) and damping capacity (DC) [1]. It is well known that the martensitic transformation of an equiatomic TiNi alloy comprises a single-stage martensitic transformation from the parent B2 phase to the B19' martensite phase. After conducting a thermomechanical treatment or adding a third element, the transformation sequence can change into a two-stage transformation, from B2 to premartensite R-phase and then to B19' upon cooling [2]. Recently, the martensitic transformation of Ni-rich TiNi SMAs was found to have more than two distinct steps, and is known as the multi-stage martensitic transformation (MST). Bataillard et al. [3,4] attributed the cause of MST to

the stress fields around coherently precipitated Ti_3Ni_4 particles. Khalil-Allafi et al. [5] found two distinct steps of $B2 \rightarrow R$ and $R \rightarrow B19'$, and an additional step with $B2 \rightarrow B19'$ in the differential scanning calorimetry (DSC) cooling curves of aged Ni-rich TiNi alloys. They proposed that the MST comes from the inhomogeneous distribution of Ti_3Ni_4 precipitates.

Su and Wu [6] have obtained a complex four-stage MST in a 20% cold-rolled and annealed $Ti_{49}Ni_{51}$ alloy, and they suggested that the MST is the result of the combined effect of severe cold-working and long-time annealing. Kim et al. [7] reported a low temperature aging-induced two-stage R-phase transformation in $Ti_{49.1}Ni_{50.9}$ alloy, and they identified that the first R-phase transformation was associated with precipitates while the second R-phase transformation could be attributed to matrix regions far from precipitates. According to the aforementioned studies, all the complex MSTs appear in Ni-rich TiNi alloys and have to do with heterogeneities caused by Ti_3Ni_4 precipitates. In this study, we find a four-stage MST in a cold-rolled and annealed $Ti_{50}Ni_{50}$ alloy. In the $Ti_{50}Ni_{50}$ alloy, neither Ti_3Ni_4 precipitation nor non-uniform precipitation

---

* Corresponding author. Address: Department of Materials Science and Engineering, National Taiwan University, 1, Roosevelt Rd., Sec. 4, Taipei 106, Taiwan, ROC. Tel.: +886 2 2363 7846; fax: +886 2 2363 4562.
  E-mail address: skw@ntu.edu.tw (S.K. Wu).

distribution is observed in the specimen. The complex MST behavior discussed in this study was identified by DSC and dynamic mechanical analyzer (DMA) tests; microstructure evidence is provided to elucidate this uncommon four-stage MST.

2. Experimental procedures

An equiatomic $Ti_{50}Ni_{50}$ alloy was prepared by conventional vacuum arc remelting. The as-melted ingots were hot-rolled at 850 °C into 2 mm thick plates, and then the plates were solution-treated at 850 °C for 2 h followed by quenching in water. The oxide layer of the solution-treated plates was removed and the specimen thickness was reduced to 1.9 mm. Thereafter, the plates were cold-rolled along the hot-rolling direction at a rolling speed of 10 m/min. No annealing process was conducted during the cold-rolling to avoid the occurrence of recrystallization. The thickness of the plate decreased from 1.9 mm to 1.24 mm and reached a final 35% thickness reduction. Then the cold-rolled plates were cut into test specimens, sealed in an evacuated quartz tube and annealed at 500 °C and 650 °C in salt baths for different time intervals.

Transformation temperatures of cold-rolled and annealed specimens were determined by DSC tests using the TA Q10 DSC equipment at a constant cooling rate (10 °C/min). Specimens for DMA experiments were cut in the direction along the rolling direction (RD). Tan δ was measured by TA 2980 DMA equipment using heating and cooling rates of 3 °C/min. The dimension of the specimens used in the DMA tests was $40 \times 5 \times 1.24$ mm^3, and the amplitude and frequency used were 2 μm and 2 Hz, respectively. The cross-sectional microstructures of the specimens were prepared by the normal metallographic procedures and then observed by a Nikon Microphoto-FXA optical microscope (OM). From the OM images, the average grain size of cold-rolled and annealed specimens was estimated by the linear intercept method [8]. Ten parallel straight lines along or normal to the rolling direction were used to count the number of grains intercepted and then the average was taken to quantify the average grain size.

3. Experimental results

3.1. DSC and DMA measurements

Fig. 1 shows the cold-rolled $Ti_{50}Ni_{50}$ alloy annealed at 500 °C for different time intervals. When the annealing time is short, as shown in Fig. 1(a) and (b), two peaks characterize the forward and reverse transformations. Upon increasing the annealing time to 1 and 3 h, the transformation occurs in four stages on cooling, as shown in Fig. 1(c) and (d). After annealing for 24 h, these four peaks combine and become two large peaks; and the two peaks in the reverse transformation after 1 and 3 h merge to one single large peak. The transformation behavior of Fig. 1 agrees with what has been reported on the transformation behavior of cold-rolled and annealed near equiatomic TiNi SMAs [9–11] except that the four-stage MST shown in Fig. 1(c) and (d) has never been reported before. As the annealing temperature is increased to 650 °C (not shown), the tendency of the transformation sequence is similar to that shown in Fig. 1. A four-stage MST also appears when the annealing is performed at 650 °C for 90 s and for longer annealing time these four peaks gradually merge to two peaks.

Fig. 2 shows DSC and DMA results of the cold-rolled specimen annealed at 500 °C for 3 h. Fig. 2(a) shows the DSC curve of Fig. 1(d) and Fig. 2(b) indicates the corresponding DMA results for tan δ. As shown in Fig. 2(b), four transformation peaks which match the transformation peaks in DSC curve are observed; there is a small shift between the results of the two methods which is attributed to different cooling/heating rates and specimen sizes used in DSC and DMA testing. In addition
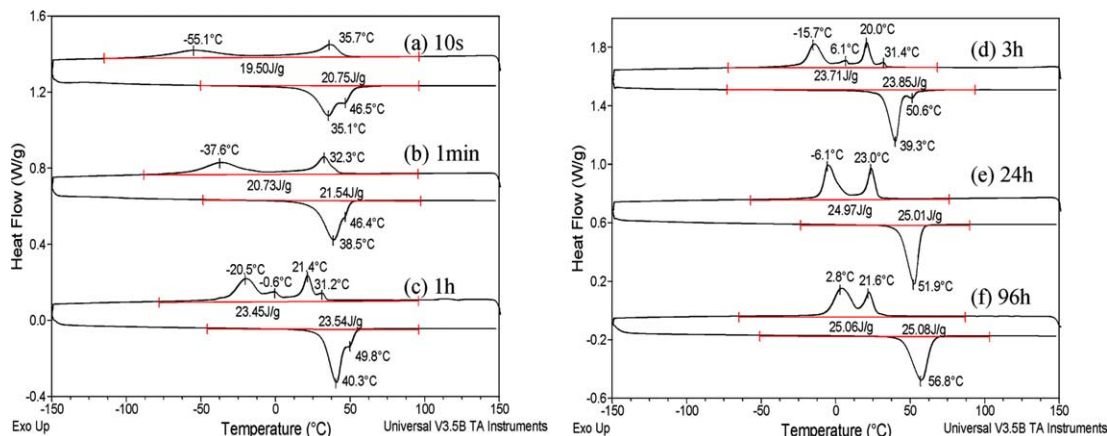

Fig. 1. DSC curves for cold-rolled $Ti_{50}Ni_{50}$ alloy annealed at 500 °C for different time intervals.

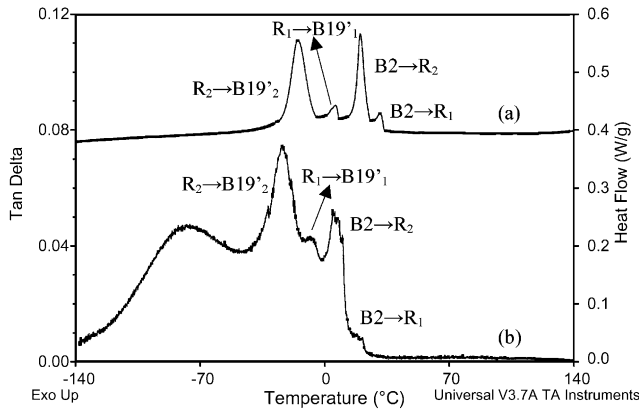Fig. 2. (a) DSC and (b) DMA curves for cold-rolled $Ti_{50}Ni_{50}$ alloy annealed at 500 °C for 3 h.

to the four transformation peaks which appear in the DSC tests, there is also one extra peak obtained at about −75 °C in Fig. 2(b). This peak was not observed in the DSC curve and is known as a relaxation peak [2].

3.2. Microstructure observations

Fig. 3 shows OM images of the cross-sectional microstructure of the cold-rolled $Ti_{50}Ni_{50}$ alloy with and without annealing at 500 °C for 3 h. Fig. 3(a) illustrates the as cold-rolled $Ti_{50}Ni_{50}$ alloy and it can readily be noticed that the microstructure in the specimen center is quite different from that near the specimen's rolling surfaces. The grains in the specimen center are elongated along the RD and the average grain size is about

40 μm. The grains near the rolling surfaces are fiber-structured and their grain boundaries are not well defined. This is because the two surfaces are in direct contact with the rollers and suffer more plastic deformation than the central region.

Fig. 3(b) shows the cross-sectional microstructure of the cold-rolled specimen annealed at 500 °C for 3 h. Fig. 3(c) and (d) show the enlarged views of the regions at the center and near the rolling surface of Fig. 3(b), respectively. The average grain sizes calculated from Fig. 3(c) and (d) are about 70 μm and 7 μm in the RD and, 15 μm and 7 μm in its normal direction, respectively. Fig. 3(e) shows the microstructure of the cold-rolled specimen annealed at 500 °C for 24 h. From Fig. 3(e), the average grain sizes in the specimen center and near the rolling surface are calculated to be about 72 μm and 53 μm in RD and 17 μm and 12 μm in its normal direction, respectively. Here, the grain sizes in the center of the sheet and that near the rolling surface are approaching each other, i.e. the grain size distribution in the whole specimen becomes more uniform.

4. Discussion

4.1. Identification of four-stage MST in a cold-rolled and annealed $Ti_{50}Ni_{50}$ alloy

4.1.1. DSC results

Fig. 4 shows several partial DSC transformation cycles of the cold-rolled specimen annealed at 500 °C for 3 h. There are four transformation peaks on cooling,
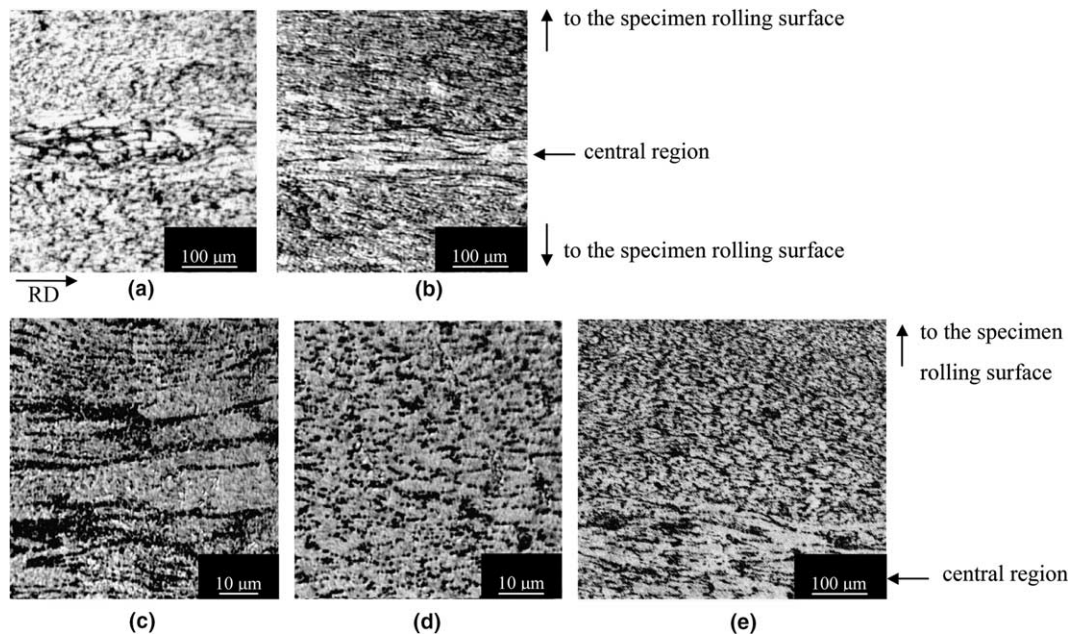

Fig. 3. OM micrographs of the cross-sections of the microstructure of cold-rolled $Ti_{50}Ni_{50}$ alloy with and without annealing: (a) as cold-rolled specimen; (b) annealed at 500 °C for 3 h; (c) enlarged central region of (b); (d) enlarged central region near the rolling surface of (b); and (e) annealed at 500 °C for 24 h.

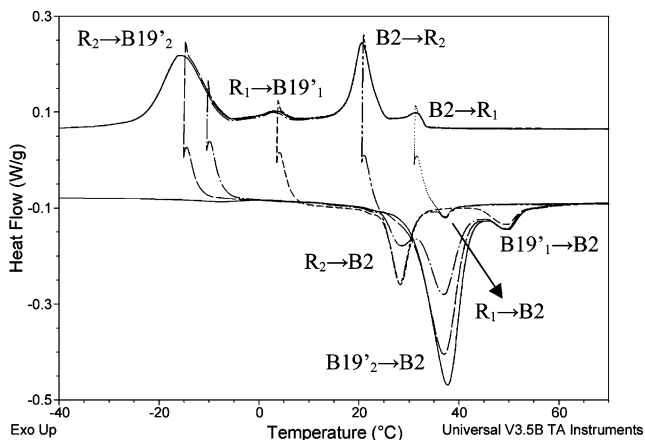Fig. 4. Overlapped partial DSC cycles for cold-rolled $Ti_{50}Ni_{50}$ alloy annealed at 500 °C for 3 h.

and we interrupt the cooling process at each transformation peak and immediately heat the specimen up to obtain the corresponding DSC heating curve. As shown in Fig. 4, the solid line represents the full DSC cycle, and the dotted line represents the DSC cycle which was interrupted at the first transformation peak (about 31.3 °C), and a new peak appears at 37.1 °C on heating which is not found in the full cycle. These two peaks are typical $B2 \leftrightarrow R_1$ due to their small hysteresis transformation temperature (about 6 °C) and small transformation enthalpies (about 1.4 J/g). Since the transformation enthalpies are lower than the normal values, 5 J/g [12], it is concluded that the transformation only takes place in a relatively small volume of the specimen. When the specimen is cooled to the second transformation peak, a peak appears at 28.2 °C on heating. Subsequently a $R_1 \rightarrow B2$ transformation peak occurs at 37.5 °C. Obviously, the new peak developed at 28.2 °C upon heating corresponds to the second transformation peak on cooling, and therefore, together with the second peak on cooling it describes $B2 \leftrightarrow R_2$ transformation characterized by a small hysteresis width and small transformation enthalpies.

When the specimen is continually cooled to the third transformation peak at about 3.8 °C, there are also two peaks observed on subsequently heating. The $R_2 \rightarrow B2$ peak is still obtained at 28.3 °C upon heating, but the $R_1 \rightarrow B2$ transformation peak at 37 °C disappears, and another new peak appears at 49.8 °C. Therefore, the third peak on cooling can be characterized as a $R_1 \rightarrow B19'_1$ transformation peak because the $R_1 \rightarrow B2$ peak disappears at 37 °C and a new $B19'_1 \rightarrow B2$ peak appears at 49.8 °C on heating. When the specimen is cooled to the fourth peak, the transformation peak of $R_2 \rightarrow B2$ at 28 °C gradually decreases and a new peak is created at about 37 °C. Consequently, the fourth peak on cooling and the new 37 °C peak on heating represent the transformations $R_2 \rightarrow B19'_2$ and $B19'_2 \rightarrow B2$, respectively.

All the transformations associated with the peaks shown in Fig. 4 are highlighted. From the figure, the transformation behavior of the cold-rolled and 500 °C × 3 h annealed $Ti_{50}Ni_{50}$ alloy is delineated as follows. When the specimen is cooled to about 31 °C, a relatively small volume transforms from B2 to R_1 first. After being cooled to 20 °C, the untransformed B2 region of the specimen starts to transform from B2 to R_2. Both R_1 and R_2 are the premartensite R-phase, but they are transformed from different regions of the specimen and R_2 is the dominant one. Upon the continuation of cooling down to 3 °C, R_1 transforms to $B19'_1$. After the temperature is cooled to −16 °C, the dominant R_2 transforms to $B19'_2$. Both $B19'_1$ and $B19'_2$ are the monoclinic martensite, but they are transformed from R_1 and R_2, respectively. During the reverse transformation on heating, $B19'_2$ and $B19'_1$ transform back to B2 at 37 °C and 50 °C, respectively. The above discussion indicates that two pairs of $B2 \rightarrow R \rightarrow B19'$ occur on cooling and two pairs of $B19' \rightarrow B2$ appear on heating.

4.1.2. DMA results

From Fig. 2(b), four $\tan \delta$ peaks at 18.1 °C, 4.5 °C, −7.2 °C and −23.4 °C correspond with four DSC transformation peaks in Fig. 2(a). It was reported that the internal friction, $Q^{-1}/\tan \delta$, of $R \leftrightarrow B19'$ transformation is much larger than that of the $B2 \leftrightarrow R$ transformation at the same strain amplitude and frequency [13]. From Section 4.1.1, peaks at 18.1 °C and 4.5 °C in Fig. 2(b) are associated with B2R and peaks at −7.2 °C and −23.4 °C are attributed to $R \rightarrow B19'$. Peak at −23.4 °C is much larger than that at 4.5 °C and peak at −7.2 °C is also much larger than that at 18.1 °C. Therefore, the DMA result of Fig. 2(b) also provides more evidence to support the four-stage MST which is comprised of two pairs of $B2R \rightarrow B19'$ on cooling, as identified in Section 4.1.1 by DSC result.

4.2. Reasons causing the four-stage MST in a cold-rolled and annealed $Ti_{50}Ni_{50}$ alloy

The reasons for the MST behavior in Ni-rich TiNi alloys have been widely discussed, and a common conclusion of this complex MST is related to the inhomogeneous formation of aging-induced Ti_3Ni_4 precipitates. However, in this study, no Ti_3Ni_4 particles precipitate in the equiatomic $Ti_{50}Ni_{50}$ specimen. Consequently, the influence of Ti_3Ni_4 precipitates and their heterogeneous precipitation on the MST behavior should be excluded.

From the DSC and DMA results in this study, the four-stage MST can only be observed in some specific annealing conditions, for example annealing at 500 °C × 1 h, 500 °C × 3 h and 650 °C × 90 s. As mentioned in Section 4.1, the four-stage MST on cooling comprises two pairs of $B2 \rightarrow R \rightarrow B19'$ transforma-

tions. OM observations in Fig. 3 show that the grain size distribution along the specimen's thickness direction is inhomogeneous, in which the grain size at the central region is apparently larger than that near the rolling surface due to the cold-rolling effect. This implies that the four-stage MST, i.e. the two pairs of $B2 \rightarrow R \rightarrow B19'$ transformations, comes from the $B2 \rightarrow R \rightarrow B19'$ transformations of grains in the central region and those of grains near the rolling surface.

In order to clarify the effect of grain size on the MST, the specimen shown in Fig. 3(b) is ground from the bottom rolling surface to remove the smaller grains in one rolling side. At the same time, the larger grains in the central region are also ground. The thickness of the specimen is now reduced from 1.2 mm to 0.4 mm. DSC test has been conducted on this ground specimen, and the result is shown in Fig. 5. Fig. 5(a) is the same specimen as Fig. 1(d), and Fig. 5(b) is the same specimen as Fig. 5(a), but now has been ground to 0.4 mm thickness. From Fig. 5(b), one can find that two small transformation peaks disappear, providing the evidence that the four-stage MST is associated with the small and large grains induced by the severely cold-rolled and annealed $Ti_{50}Ni_{50}$ alloy. In other words, in Fig. 5(a), two small peaks on cooling are associated with $B2 \rightarrow R \rightarrow B19'$ caused by large grains in the central region of the specimen, but two large peaks on cooling, although they are also associated with $B2 \rightarrow R \rightarrow B19'$, are caused from small grains near the rolling surface of the specimen.

The reason why the transformation peaks corresponding to larger grains are smaller than those corresponding to smaller grains comes from the fact that the volume of large grains in the central region is less than that of small grains near the rolling surface. This is because the thickness of large grains in the specimen center is only about 50–100 μm, which is comparatively less than the whole specimen thickness of about 1200 μm.

From the viewpoint of the cold-rolling effect, the degree of plastic deformation at the specimen center should be much less than the 35% thickness reduction of the whole specimen. As a result, the recrystallized grains in the central region should be larger than those near the rolling surface under the same annealing condition. At the same time, defects and dislocations induced by the severe cold-rolling of grains near the specimen's surface should be much more than those in the center. It is well known that these cold-rolling induced defects/dislocations can suppress premartensitic and martensitic transformations to lower temperatures [9]. Therefore, $B2 \rightarrow R$ and $R \rightarrow B19'$ transformations corresponding to small grains on cooling take place at lower temperatures than those corresponding to large grains, as shown in Fig. 5.

5. Conclusions

The transformation behavior of $Ti_{50}Ni_{50}$ shape memory alloy after 35% cold-rolling and subsequent recrystallization annealing is investigated in this study. The four-stage MST appears at specific annealing conditions having two large and two small peaks in the cooling curves of DSC and DMA $\tan \delta$ tests. Microstructural observations reveal that the grain size distribution along the specimen's thickness direction is inhomogeneous due to the cold rolling effect, in which the grain size at the central region is apparently larger than that near the rolling surface. Two small peaks in four-stage MST are related to the $B2 \rightarrow R \rightarrow B19'_1$ transformations of large grains and two large peaks are also associated with the $B2 \rightarrow R \rightarrow B19'$ transformations, but now they correspond to small grains near the rolling surface. The volume of large grains in the specimen center is much less than that of small grains near the rolling surface. This feature accounts for the appearance of two small and two large peaks on cooling.
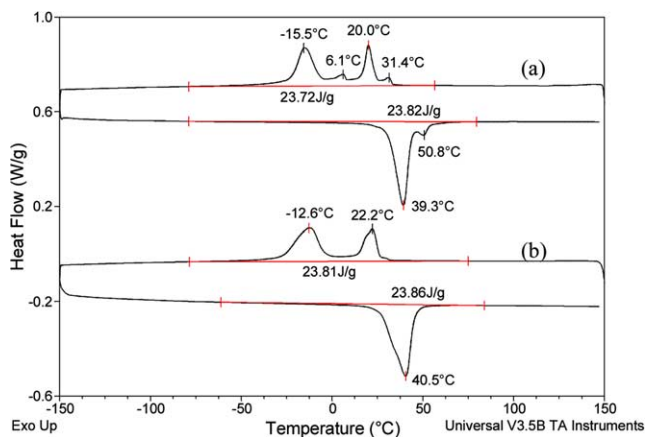
Fig. 5. DSC curves for cold-rolled $Ti_{50}Ni_{50}$ alloy annealed at 500 °C for 3 h: (a) original specimen with 1.2 mm thickness (the same as Fig. 1(d)); (b) ground specimen to 0.4 mm thickness.

References

[1] Wayman CM, During TW. In: During TW, Melton KN, Stöckel D, Wayman CM, editors. Engineering aspects of shape memory alloys. London: Butterworth-Heinemann; 1990. p. 3–20.
[2] Wu SK, Lin HC, Chou TS. Acta Metall Mater 1990;38:95.
[3] Bataillard L, Gotthardt R. J Phys III 1995;5:C8–C647.
[4] Bataillard L, Bidaux J-E, Gotthardt R. Philos Mag 1998;78:327.
[5] Khalil-Allafi J, Dlouhy A, Eggeler G. Acta Mater 2002;50:4255.

[6] Su PC, Wu SK. Acta Mater 2004;52:1117.

[7] Kim JI, Liu Y, Miyazaki S. Acta Mater 2004;52:487.

[8] ASTM Standards—Standards test method for determining average grain size. Annual book of ASTM standards, vol. 03.01. 2003. p. 256.

[9] Khelfaoui F, Guénin G. Mater Sci Eng A 2003;355:292.

[10] Thoma PE, Kao MY, Fariabi S, AbuJudom DN. In: Proceedings of ICOMAT 92. p. 917.

[11] Treppmann D, Hornbogen E, Wurzel D. In: Proceedings of ICOMAT 95. p. C8-569.

[12] Lin HC, Wu SK. Scripta Metall Mater 1991;25:1295.

[13] Lin HC, Wu SK, Yeh MT. Metall Trans A 1993;24:2189.